Sensitivity of simulated extent and future evolution of marine suboxia to mixing intensity

O. Duteil[1] and A. Oschlies[1]

[1] Geological and hydrographic records contain evidence of substantial past variations in the oxygenation of the global ocean. Numerical models predicts a future decrease of marine oxygen levels under global warming. Using a global biogeochemical-climate model in which diapycnal mixing is parametrised as the sum of the regionally heterogenous tidal and homogenous background vertical mixing, we here show that simulated total oceanic oxygen content and the extent of marine suboxia are both sensitive to the strength of background vertical mixing. Eight otherwise identical configurations of the model were spun up under pre-industrial conditions for different vertical diffusivities ranging from background values of 0.01 cm^2/s to 0.5 cm^2/s. This range corresponds to various observational estimates and to values currently used in numerical ocean circulation models. Whereas the simulated total oceanic oxygen content is larger for larger mixing intensities, the simulated suboxic volume displays a maximum at intermediate diffusivities of about 0.2 cm^2/s. The intensity of vertical mixing also determines the evolution of suboxic areas under projected 21st century CO_2 emissions: while all model configurations predict a decline in total oceanic oxygen, the simulated extent of marine suboxia shows a 21st century expansion only for mixing rates higher than 0.2 cm^2/s, whereas the suboxic volume declines for lower mixing rates despite an overall loss of marine oxygen. Differences in the poorly constrained mixing parameterisation can thus lead to qualitatively different estimates about the future evolution of marine suboxia under projected climate change. **Citation:** Duteil, O., and A. Oschlies (2011), Sensitivity of simulated extent and future evolution of marine suboxia to mixing intensity, *Geophys. Res. Lett.*, *38*, L06607, doi:10.1029/2011GL046877.

1. Introduction

[2] Oxygen is produced by photosynthesis in the surface waters, and quickly equilibrates with the atmosphere across the sea surface. In the dark ocean interior, oxygen is consumed during remineralization of organic matter exported from the euphotic surface layer. The only way to supply oxygen from the well ventilated surface layer to the ocean interior is via physical transport processes. Because the downward organic matter flux declines with depth, oxygen utilization also generally decreases with depth. As a result, oxygen concentrations are generally lower in intermediate waters (100 to 1000 m deep) than in the surface waters

above and in the deep waters below [*Wyrtki*, 1962]. This picture is carried to extremes in areas where sluggish circulation and high primary productivity in overlying surface waters cause subsurface oxygen concentrations to drop to near zero. In today's ocean, major suboxic regions (here defined by $[O_2] < 5$ μM) exist in the Arabian Sea and in the tropical Pacific Ocean. Their total volume has been estimated as 0.46×10^{15} m^3 [*Karstensen et al.*, 2008]. Although covering only a small fraction (0.35%) of the global ocean volume, suboxic areas are of global biogeochemical significance because they are associated with a loss of fixed nitrogen from the ocean via denitrification and anaerobic ammonium oxidation (anammox).

[3] The potential sensitivity of low-oxygen areas to climate change has been investigated with Ocean General Circulation Models [*Bopp et al.*, 2002; *Oschlies et al.*, 2008; *Matear and Hirst*, 2003]. However, such models still have substantial difficulties in adequately reproducing observed oxygen distributions. Simulated oxygen fields differ considerably among the different circulation models [*Najjar et al.*, 2007] and different biogeochemical models [*Meissner et al.*, 2005]. A key parameter that controls both ocean circulation and biogeochemical cycles is the intensity of diapycnal mixing in the ocean interior [*Bryan*, 1987]. For example, the simulated strength of the Meridional Overturning Circulation (MOC) depends directly on ocean-interior mixing rates and increases with vertical diffusivity [*Prange et al.*, 2003]. An increase with vertical mixing is also found for simulated new production and export production [*Oschlies*, 2001].

[4] Observational estimates of the vertical diffusivity vary by more than an order of magnitude. Inferences from the large-scale density structure of the global ocean suggest that the global average diapycnal diffusivity is of the order of 1 cm^2/s [*Munk and Wunsch*, 1998]. However, local estimates derived from microstructure measurements and tracer release experiments [*Ledwell et al.*, 1998] yield values ranging from 0.1 to 0.5 cm^2/s in the ocean interior, though much larger values are observed in regions of elevated internal wave energy, particularly near steeply sloping topography. As a consequence of the still not fully understood spatial variability in diapycnal mixing rates, mixing parameterisations vary considerably among different models and result in vertical diffusivities employed in the stably stratified thermocline ranging from 0.01 cm^2/s [*Duteil et al.*, 2009] to 0.3 cm^2/s [*Matear and Hirst*, 2003]. Here, we investigate the sensitivity of simulated suboxic regions to variations of diapycnal diffusivities.

2. Model

[5] The model used in this study is the University of Victoria (UVic) Earth System Climate Model [*Weaver et al.*,

---

[1]Leibniz-Institut für Meereswissenschaften an der Universität Kiel (IFM-GEOMAR), Kiel, Germany.
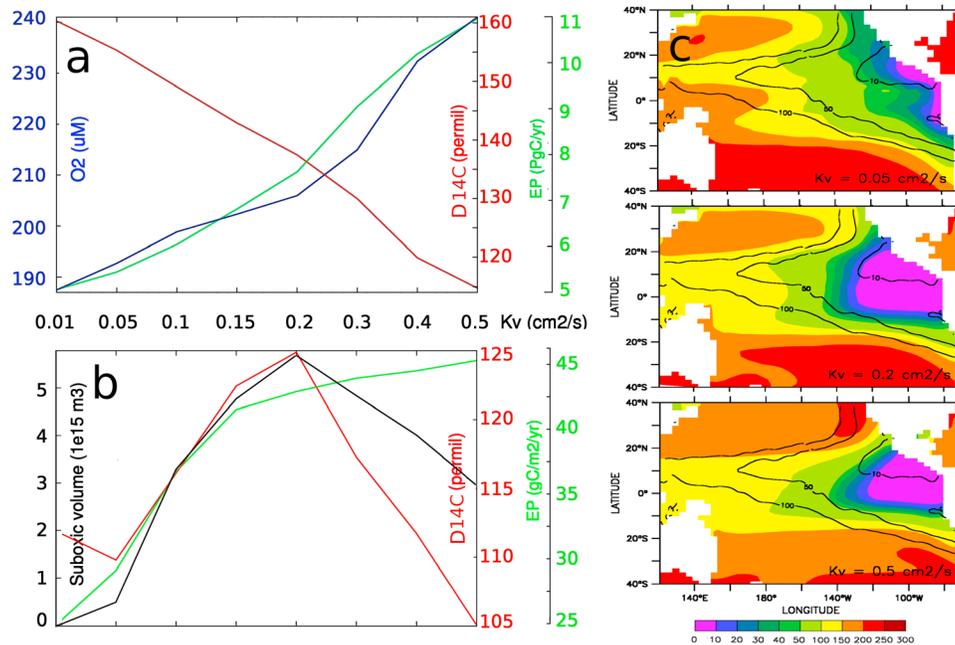
Figure 1. (a) Simulated global mean of oxygen concentration (μM), negative D14C anomaly (permil), and particulate organic carbon export (PgC/yr) as a function of the vertical background diffusivity applied in the respective model experiments. (b) Simulated suboxic (threshold 5 μM) volume (1e15 m^3), mean export production (gC/yr/m^2) and negative D14C anomaly (permil) over the region 120–80W, 10S–20N, 0–1000 m as a function of vertical background diffusivities. (c) Oxygen concentrations (μM) at 500 m depth for experiments (year 2000) using a vertical background diffusivity K_{vbg} of (top) 0.05 cm^2/s, (middle) 0.2 cm^2/s and (bottom) 0.5 cm^2/s. The black contours refer to the 10, 50 and 100 μM levels from the World ocean Atlas.

2001] version 2.8. The oceanic component is a fully three dimensional primitive-equation model with nineteen levels in the vertical and a horizontal resolution of 1.8 degree latitude × 3.6 degree longitude. It contains a simple marine ecosystem model with the two nutrients nitrate and phosphate and two phytoplankton classes, nitrogen fixers. and other phytoplankton. The trace nutrient iron is not explicitly included in the model. Nevertheless, a reasonable fit to observed biogeochemical tracer distributions can be achieved [*Schmittner et al.*, 2008; *Oschlies et al.*, 2008] and the combination of relatively low phytoplankton growth and high maximum zooplankton grazing allows for the presence of substantial levels of macronutrients in the model's surface layers of the tropical eastern Pacific. As iron is mostly provided to this area by upwelling, changes in upwelling can be expected to affect the supply of iron in ways qualitatively similar to the supply of macronutrients.

[6] Diapycnal mixing K_v is parameterized as the sum of tidally induced mixing K_{vtidal} and background mixing K_{vbg}. The tidally induced diffusivity rapidly decays in the water column above the seafloor with an exponential vertical scale of 500 m [*Simmons et al.*, 2004]. As a result, the background diffusivity determines the value of diapycnal mixing in most parts of the pycnocline and oxygen minimum zones. This mixing background is assumed constant within each experiment. It is set to K_{vbg} = 0.01, 0.05, 0.1, 0.15, 0.2, 0.3, 0.4 and 0.5 cm^2/s in the eight sensitivity runs, respectively. South of 40°S, a value of 1 cm^2/s is added to the background diffusivity in the entire water column to account for observed vigorous mixing in the Southern Ocean [*Naveira Garabato et al.*, 2004; *Goes et al.*, 2010]. Each experiment is spun up for 10,000 years under preindustrial

atmospheric and astronomical boundary conditions, before being run under historical conditions from 1765 to 2000 [*Schmittner et al.*, 2008]. From 2000 to 2100, each model is forced by CO_2 emissions following the SRES A2 scenario, leading to an increase from today's emissions of about 8 Gt C yr^{-1} to about 29 Gt C yr^{-1} in 2100.

3. Results

[7] Across the range of model configurations differing only in the applied vertical diffusivity, simulated global-mean marine oxygen concentrations increase with increasing vertical diffusivity K_{vbg} from 185 μM for K_{vbg} = 0.01 cm^2/s to 240 μM for K_{vbg} = 0.5 cm^2/s (Figure 1a). This behaviour is related to increased ventilation via an enhanced overturning circulation, as shown by the closely correlated decrease of global-mean water D14C anomaly of −160 per mil for K_{vbg} = 0.01 cm^2/s, to −115 per mil for K_{vbg} = 0.5 cm^2/s. The systematic trends in mean oxygen concentrations and mean D14C reservoir age over the entire range of diffusivities suggest that even for the lowest diffusivities used, implicit numerical diffusion does not dominate the effective mixing felt by the simulated tracer fields.

[8] Enhanced mixing also leads to enhanced supply of nutrients to the surface waters and to an associated increase in simulated export production, here defined as all particulate organic carbon export across a depth of 125 m, which increases from 5 GtC/yr for K_{vbg} = 0.01 cm^2/s to 11.0 GtC/yr for K_{vbg} = 0.5 cm^2/s. Although enhanced export production leads to enhanced respiratory oxygen consumption in the ocean interior, the net effect of increased vertical mixing is an increase in the global oceanic oxygen content. This finding
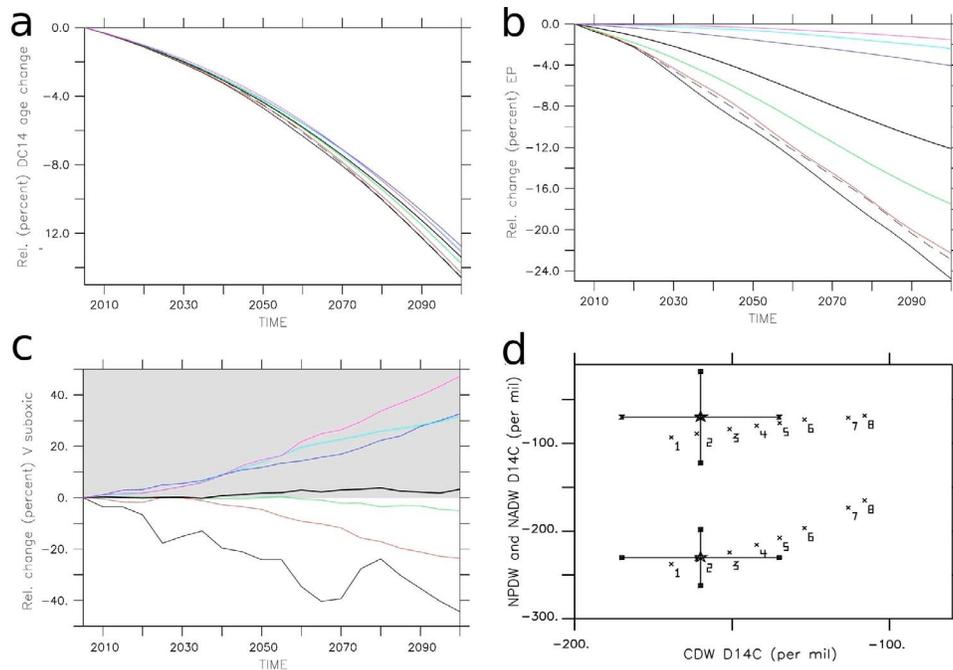
Figure 2. Simulated evolution of (a) D14C, (b) export production, and (c) suboxic volume (threshold 5 μM) over the region 120–80W, 10S–20N. For each simulation, this evolution is expressed in relative percent change using year 2000 as reference. Experiments with different background diffusivities are represented by different colors (dots: 0.01 cm^2/s, black: 0.05 cm^2/s, red: 0.1 cm^2/s, green: 0.15 cm^2/s, bold black: 0.2 cm^2/s, deep blue: 0.3 cm^2/s, cyan: 0.4 cm^2/s, pink: 0.5 cm^2/s). (d) Observed and modelled deep D14C averaged for North Atlantic Deep Water (NADW, 1000–3500 m, 0–60°N of Atlantic basin), North Pacific Deep Water (NPDW, 1500–5000 m, 0–60°N of Pacific basin), and Circumpolar Deep Water (CDW, 1500–5000 m, south of 45°S), following *Matsumoto et al.* [2004]. Symbols with error bars (2 standard deviations) are observations. Dots represent models configurations (1: K_{vbg} = 0.01 cm^2/s, 2: 0.05 cm^2/s, 3: 0.1 cm^2/s, 4: 0.15 cm^2/s, 5: 0.2 cm^2/s, 6: 0.3 cm^2/s, 7: 0.4 cm^2/s, and 8: 0.5 cm^2/s).

agrees with results from earlier carbon-climate model studies [*Bopp et al.*, 2002; *Matear and Hirst*, 2003; *Schmittner et al.*, 2008] that revealed a 4 to 7 percent decrease in average oxygen concentrations until the end of the century, caused mainly by a slowdown in circulation with only about 25% attributed to a warming-induced decrease in oxygen solubility [*Bopp et al.*, 2002; *Matear and Hirst*, 2003].

[9] The tropical Pacific contains the largest low-oxygen area both in the model and in the real ocean (Figure 1c). Rather counterintuitively, the simulated suboxic water volume does not steadily decrease with increasing diffusivities, but instead shows a maximum for intermediate mixing rates (K_{vbg} = 0.2 cm^2/s, Figure 1b). The suboxic volume decreases by about 90% for a lower value of K_{vbg} = 0.05 cm^2/s and by about 50% for a higher value of K_{vbg} = 0.5 cm^2/s compared to the maximum obtained for K_{vbg} = 0.2 cm^2/s. Suboxia does not develop in tropical Pacific when K_{vbg} = 0.01 cm^2/s. The relatively coarse resolution of the model grid does not allow for a correct representation of the equatorial current system. As a result, the simulated suboxic volume, which ranges from 0.5 × 10^{15} to 5 × 10^{15} m^3, exceeds the observational estimate of 0.46 × 10^{15} m^3 [*Karstensen et al.*, 2008]. This discrepancy might partly be explained by sampling and interpolation issues of the observational data sets [*Fuenzalida et al.*, 2009].

[10] Simulated export production averaged over the region 120–80°W and 10°S–20°N that contains the Pacific suboxic area increases with K_{vbg} from 25 gC/m^2/yr for K_{vbg} = 0.01 cm^2/s to 45 gC/m^2/yr for K_{vbg} = 0.5 cm^2/s. When

mixing is strong, large amounts of nutrients are supplied to the euphotic zone, leading to high export production and oxygen consumption. At the same time, high ventilation rates and associated oxygen supply more than compensate for the elevated biotic oxygen consumption, yielding a decline in suboxic volume with increasing mixing rates (Figure 1b). This is consistent with an analysis of radiocarbon concentrations simulated for the same area (120–80°W, 10°S–20°N) and the upper 1000 m. Concentrations of D14C are relatively high (-around 110 per mil) for low values of K_{vbg} due to ventilation by downwelled thermocline water, reach more negative values (−125 per mil) representative of older water at intermediate diffusivities, and again higher ones (−105 per mil) when K_{vbg} is large and the meridional overturning is more vigorous (Figure 1b). A predominant control of the suboxic water volume by ocean dynamics rather than local export production and remineralisation has also been inferred from previous studies [*Meissner et al.*, 2005; *Galbraith et al.*, 2004].

[11] How may the volume of suboxic waters change in the future? Model results suggest that increased greenhouse gas concentrations and associated high-latitude warming and freshening will weaken the MOC [*Gregory et al.*, 2005]. Enhanced stratification leads to younger ocean surface waters because of reduced mixing with deeper and older waters [*Gnanadesikan et al.*, 2007]. In the model used here, the mean D14C age in the upper (0–1000 m) eastern tropical Pacific (120–80°W, 10°S–20°N) decreases by about 13 to 14% by the year 2100 for all mixing coefficients (Figure 2a).

Enhanced stratification also tends to reduce the supply of nutrients to the surface ocean and, thereby, reduces export production. For high vertical diffusivities ($K_{vbg} = 0.5$ cm^2/s), simulated export production decreases by about 2% from year 2000 to 2100 in the eastern tropical Pacific (Figure 2c). The relative decrease is larger and amounts to some 25% for small diffusivities (0.05 cm^2/s).

[12] All model configurations show a decrease of the total oceanic oxygen under global warming (Figure 2c). Reduced ventilation causes a decrease in mean oxygen concentrations, with a small contribution from decreased oxygen solubility in warmer surface waters [*Matear and Hirst*, 2003]. A decrease in oxygen concentrations has in many places been observed during the last decades [*Stramma et al.*, 2008]. In our numerical model configurations, the mean oxygen concentration is already 1 to 2% smaller in year 2000 compared to preindustrial time. This value is nearly independent of the vertical diffusivity. By year 2100, simulated global-mean oxygen values are further reduced by another 3 to 3.5%, consistent with the results of earlier model studies [*Bopp et al.*, 2002; *Matear and Hirst*, 2003; *Oschlies et al.*, 2008].

[13] Oxygen concentrations will, however, not decline everywhere. Model studies have already suggested that tropical thermocline waters may become younger under global warming as a result of altered balance of lateral advective ventilation and reduced vertical mixing of older waters from below [*Gnanadesikan et al.*, 2007]. The same change in transport pathways might also lead to increasing oxygen concentrations in the tropical thermocline under global warming. This is consistent with earlier results obtained with the UVic model used here: For constant carbon-to-nutrient ratios in the cycling of organic matter, simulated oxygen concentrations in the tropical thermocline showed an increase over the 21st century, while an expansion of suboxic areas was simulated only when a hypothetical CO_2-dependent increase in carbon-to-nitrogen ratios of organic matter was assumed [*Oschlies et al.*, 2008]. The current study assumes constant elemental ratios in all model configurations.

[14] Results of the different models run with different vertical diffusivities reveal expanding 21st century suboxia for high mixing intensities, whereas suboxic volumes shrink for low diffusivities (Figure 2c). More specifically, for $K_{vbg} = 0.5$ cm^2/s, the suboxic volume increases by 50% between years 2000 and 2100. When K_{vbg} is ten times smaller, the suboxic volume instead decreases by about 45% over the same time span. For an intermediate value of $K_{vbg} = 0.15$ cm^2/s, a relatively small decrease in the suboxic volume by 5% is simulated. At low mixing intensities, the global-warming induced relative decline in export production (Figure 2b) is larger than the relative decrease in D14C age (Figure 2a), resulting in an increase in oxygen concentrations in the model's tropical thermocline and an associated reduction in the suboxic volume. In contrast, the relative 21st century's decline in export production is slower at high mixing rates, and the general slow-down in ocean overturning leads to a decline in tropical oxygen concentrations and an associated expansion of the suboxic regions in the model. In this study, changes in suboxic volume have been considered only for the 21st century. Results may differ on longer timescales. For example, the simulation of *Schmittner et al.* [2008] showed relatively little change in suboxic volume from 2000 to 2100, with a significant 30% increase

beginning only at the end of the 21st century and reaching a plateau after year 2500.

4. Discussion

[15] The significance of the results presented above depends on how realistic the circulation and tracer fields of the various model configurations are. Previous studies using the same model employed a background diffusivity of $K_{vbg} = 0.15$ cm^2/s [*Oschlies et al.*, 2008; *Schmittner et al.*, 2008]. The biological model parameters were tuned to achieve a reasonable fit to observed marine biogeochemical tracer distributions including suboxic regions [*Schmittner et al.*, 2008]. The generally good agreement with CFC and radiocarbon data indicates that the simulated ventilation patterns on multidecadal to millennial timescales are well represented in the model using a K_{vbg} of 0.15 cm^2/s [*Goes et al.*, 2010].

[16] This is consistent with our assessment of the realism of these different configurations using the D14C-based metric as defined by *Matsumoto et al.* [2004]. Results of this metric are displayed in Figure 2d for the different model configurations and indicate that only values of K_{vbg} lower than 0.2 cm^2/s yield D14C distributions within the observational error bars. According to these model configurations, the simulated suboxic volume either stays constant or shrinks over the 21st century under a business-as-usual emission scenario and the assumption of constant elemental stoichiometry (Figure 2c).

5. Conclusions

[17] A series of simulations with a coupled biogeochemical-climate model differing only in the applied vertical diffusivities have shown that the simulated extent of marine suboxia is very sensitive to the specific choice of the mixing parameters within the range of observational estimates. A maximum extent of suboxic waters is simulated for intermediate background diffusivities of 0.2 cm^2/s, whereas both higher and lower mixing rates lead to smaller suboxic volumes. One implication of the results shown here is that a stagnant ocean (zero mixing) is unlikely to give rise to suboxic or even anoxic conditions, because it lacks the necessary nutrient supply and associated export production to sustain sufficiently high rates of oxygen consumption in the ocean interior. Results of our model suggest further that under a business-as-usual scenario, the same CO_2-emission can even lead to opposite trends in the simulated future evolution of the ocean's suboxic volume, depending on the assumptions made about the vertical mixing rate. Best agreement with observed D14C distributions is found for mixing parameterisations that yield a steady or declining suboxic volume under a business-as-usual emission scenario over the 21st century despite a decline in the total oceanic oxygen inventory. Further studies will have to investigate the sensitivity of these results to improved mechanistic descriptions of diapycnal mixing in the ocean.

[19] The Editor thanks one anonymous reviewer for their assistance in evaluating this paper.

References

Bopp, L., C. Le Quéré, M. Heimann, A. C. Manning, and P. Monfray (2002), Climate-induced oceanic oxygen fluxes: Implications for the contemporary carbon budget, *Global Biogeochem. Cycles*, *16*(2), 1022, doi:10.1029/2001GB001445.

Bryan, F. (1987), Parameter sensitivity of primitive equation ocean general circulation models, *J. Phys. Oceanogr.*, *17*(7), 970–985.

Duteil, O., A. Lazar, Y. Dandonneau, I. Wainer, and C. Menkes (2009), Deep chlorophyll maximum and upper ocean structure interactions: Case of the Guinea thermal dome, *J. Mar. Res.*, *67*(2), 239–271.

Fuenzalida, R., W. Schneider, J. Garces-Vargas, L. Bravo, and C. Lange (2009), Vertical and horizontal extension of the oxygen minimum zone in the eastern South Pacific Ocean, *Deep Sea Res., Part II*, *56*(16), 1027–1038, doi:10.1016/j.dsr2.2008.11.001.

Galbraith, E. D., M. Kienast, T. F. Pedersen, and S. E. Calvert (2004), Glacial-interglacial modulation of the marine nitrogen cycle by high-latitude O_2 supply to the global thermocline, *Paleoceanography*, *19*, PA4007, doi:10.1029/2003PA001000.

Gnanadesikan, A., J. Russell, and F. Zeng (2007), How does ocean ventilation change under global warming?, *Ocean Sci.*, *3*(1), 43–53.

Goes, M., N. M. Urban, R. Tonkonojenkov, M. Haran, A. Schmittner, and K. Keller (2010), What is the skill of ocean tracers in reducing uncertainties about ocean diapycnal mixing and projections of the Atlantic Meridional Overturning Circulation?, *J. Geophys. Res.*, *115*, C12006, doi:10.1029/2010JC006407.

Gregory, J. M., et al. (2005), A model intercomparison of changes in the Atlantic thermohaline circulation in response to increasing atmospheric CO_2 concentration, *Geophys. Res. Lett.*, *32*, L12703, doi:10.1029/2005GL023209.

Karstensen, J., L. Stramma, and M. Visbeck (2008), Oxygen minimum zones in the eastern tropical Atlantic and Pacific oceans, *Prog. Oceanogr.*, *77*(4), 331–350, doi:10.1016/j.pocean.2007.05.009.

Ledwell, J. R., A. J. Watson, and C. S. Law (1998), Mixing of a tracer in the pycnocline, *J. Geophys. Res.*, *103*(C10), 21,499–21,529.

Matear, R. J., and A. C. Hirst (2003), Long-term changes in dissolved oxygen concentrations in the ocean caused by protracted global warming, *Global Biogeochem. Cycles*, *17*(4), 1125, doi:10.1029/2002GB001997.

Matsumoto, K., et al. (2004), Evaluation of ocean carbon cycle models with data-based metrics, *Geophys. Res. Lett.*, *31*, L07303, doi:10.1029/2003GL018970.

Meissner, K. J., E. D. Galbraith, and C. Vlker (2005), Denitrification under glacial and interglacial conditions: A physical approach, *Paleoceanography*, *20*, PA3001, doi:10.1029/2004PA001083.

Munk, W., and C. Wunsch (1998), Abyssal recipes II: Energetics of tidal and wind mixing, *Deep Sea Res., Part I*, *45*(12), 1977–2010.

Najjar, R. G., et al. (2007), Impact of circulation on export production, dissolved organic matter, and dissolved oxygen in the ocean: Results from Phase II of the Ocean Carbon-cycle Model Intercomparison Project (OCMIP-2), *Global Biogeochem. Cycles*, *21*, GB3007, doi:10.1029/2006GB002857.

Naveira Garabato, A. C., K. L. Polzin, B. A. King, K. J. Heywood, and M. Visbeck (2004), Widespread intense turbulent mixing in the Southern Ocean, *Science*, *303*, 210–213.

Oschlies, A. (2001), Model-derived estimates of new production: New results point towards lower values, *Deep Sea Res., Part II*, *48*(10), 2173–2197.

Oschlies, A., K. G. Schulz, U. Riebesell, and A. Schmittner (2008), Simulated 21st century's increase in oceanic suboxia by CO_2-enhanced biotic carbon export, *Global Biogeochem. Cycles*, *22*, GB4008, doi:10.1029/2007GB003147.

Prange, M., G. Lohmann, and A. Paul (2003), Influence of vertical mixing on the thermohaline hysteresis: Analyses of an OGCM, *J. Phys. Oceanogr.*, *33*(8), 1707–1721.

Schmittner, A., A. Oschlies, H. D. Matthews, and E. D. Galbraith (2008), Future changes in climate, ocean circulation, ecosystems, and biogeochemical cycling simulated for a business-as-usual CO_2 emission scenario until year 4000 AD, *Global Biogeochem. Cycles*, *22*, GB1013, doi:10.1029/2007GB002953.

Simmons, A. L., S. R. Jayne, L. C. St Laurent, and A. J. Weaver (2004), Tidally driven mixing in a numerical model of the ocean general circulation, *Ocean Modell.*, *6*, 245–263.

Stramma, L., G. Johnson, J. Sprintall, and V. Mohrholz (2008), Expanding oxygen-minimum zones in the tropical oceans, *Science*, *320*(5876), 655–658, doi:10.1126/science.1153847.

Weaver, A., et al. (2001), The UVic Earth System Climate Model: Model description, climatology, and applications to past, present and future climates, *Atmos. Ocean*, *39*(4), 361–428.

Wyrtki, K. (1962), The oxygen minima in relation to ocean circulation, *Deep Sea Res.*, *9*(1), 11–23.

O. Duteil and A. Oschlies, Leibniz-Institut für Meereswissenschaften an der Universität Kiel (IFM-GEOMAR), Duesternbrooker Weg 20, D-24105 Kiel, Germany. (oduteil@ifm-geomar.de)